

Mutations in the C-Terminal Domain of ColQ in Endplate Acetylcholinesterase Deficiency Compromise ColQ–MuSK Interaction

Tomohiko Nakata,^{1,2} Mikako Ito,¹ Yoshiteru Azuma,^{1,2} Kenji Otsuka,¹ Yoichiro Noguchi,¹ Hirofumi Komaki,³ Akihisa Okumura,⁴ Kazuhiro Shiraishi,⁵ Akio Masuda,¹ Jun Natsume,² Seiji Kojima,² and Kinji Ohno^{1*}

¹Division of Neurogenetics Center for Neurological Diseases and Cancer, Nagoya University Graduate School of Medicine, Nagoya, Japan;

²Department of Pediatrics Nagoya University Graduate School of Medicine, Nagoya, Japan; ³Department of Child Neurology National Center

Hospital, National Center of Neurology and Psychiatry (NCNP), Tokyo, Japan; ⁴Department of Pediatrics Juntendo University Faculty of Medicine,

Tokyo, Japan; ⁵Department of Pediatrics Utano National Hospital, Kyoto, Japan

Communicated by Lars Bertram

Received 19 January 2013; accepted revised manuscript 19 March 2013.

Published online 29 March 2013 in Wiley Online Library (www.wiley.com/humanmutation). DOI: 10.1002/humu.22325

ABSTRACT: Acetylcholinesterase (AChE) at the neuromuscular junction (NMJ) is mostly composed of an asymmetric form in which three tetramers of catalytic AChE subunits are linked to a triple helical collagen Q (ColQ). Mutations in COLQ cause endplate AChE deficiency. We report three patients with endplate AChE deficiency with five recessive COLQ mutations. Sedimentation profiles showed that p.Val322Asp and p.Arg227X, but not p.Cys444Tyr, p.Asp447His, or p.Arg452Cys, inhibit formation of triple helical ColQ. In vitro overlay of mutant ColQ-tailed AChE on muscle sections of Colq^{-/-} mice revealed that p.Cys444Tyr, p.Asp447His, and p.Arg452Cys in the C-terminal domain (CTD) abrogate anchoring ColQ-tailed AChE to the NMJ. In vitro plate-binding assay similarly demonstrated that the three mutants inhibit binding of ColQ-tailed AChE to MuSK. We also confirmed the pathogenicity of p.Asp447His by treating Colq^{-/-} mice with adeno-associated virus serotype 8 carrying mutant COLQ-p.Asp447His. The treated mice showed no improvement in motor functions and no anchoring of ColQ-tailed AChE at the NMJ. Electroporation of mutant COLQ harboring p.Cys444Tyr, p.Asp447His, and p.Arg452Cys into anterior tibial muscles of Colq^{-/-} mice similarly failed to anchor ColQ-tailed AChE at the NMJ. We proved that the missense mutations in ColQ–CTD cause endplate AChE deficiency by compromising ColQ–MuSK interaction at the NMJ.

Hum Mutat 34:997–1004, 2013. © 2013 Wiley Periodicals, Inc.

KEY WORDS: COLQ; collagen Q; neuromuscular; acetylcholinesterase; myasthenic syndromes

Introduction

Congenital myasthenic syndromes (CMS) are clinically and genetically heterogeneous inherited disorders characterized by neuromuscular transmission defect caused by mutations affecting proteins expressed at the neuromuscular junction (NMJ) [Engel et al., 2003]. The synaptic type of CMS is caused by the absence of the asymmetric form of acetylcholinesterase (AChE) from the endplate [Engel et al., 1977]. Endplate AChE deficiency is characterized by generalized muscle weakness, fatigue, scoliosis, minor facial abnormalities, and episodes of respiratory distress [Mihaylova et al., 2008]. In the absence of AChE, the duration of the endplate currents are prolonged, so that it outlasts the refractory period of the skeletal muscle sodium channel, which in turn evokes repetitive compound muscle action potentials (CMAPs). Four mechanisms lead to defective neuromuscular signal transmission in endplate AChE deficiency [Engel et al., 1977; Ohno et al., 1998]. First, the prolonged endplate currents lead to overload of Ca²⁺ ions at the postsynaptic sarcoplasm, which causes endplate myopathy with loss of acetylcholine receptor (AChR). Second, excessive ACh at the synaptic space causes desensitization of AChR. Third, repeated opening of AChR causes staircase summation of endplate potentials, which depolarizes the resting membrane potential and makes the muscle sodium channel irresponsive to an endplate potential. Fourth, lack of ColQ at the NMJ diminishes the amount of membrane-bound MuSK and reduces phosphorylation of the AChR β subunit, which compromises AChR clustering [Sigoillot et al., 2010]. Lack of effects of cholinesterase inhibitors, or even worsening of the symptoms with them, in patients with endplate AChE deficiency suggests that lack of AChE rather than lack of AChR is a key underlying mechanism leading to myasthenic symptoms.

Endplate AChE deficiency is not caused by mutations in the AChE gene (NM_000665.3; MIM #100740) encoding the catalytic subunit but is caused by recessive mutations in the COLQ gene (NM_005677.3; MIM #603033) encoding the collagenic tail subunit [Ohno et al., 1998]. There are two major types of AChE in the skeletal muscle: (1) globular forms consisting of monomers (G₁), dimers (G₂), or tetramers (G₄) of the T isoform of the catalytic subunit (AChE_T, NP_000656.1), and (2) asymmetric forms consisting of one, two, or three homotetramers (A₄, A₈ and A₁₂, respectively) of AChE_T attached to a triple-stranded collagenic tail (ColQ) [Massoulié, 2002], which are hereafter called ColQ-tailed

Additional Supporting Information may be found in the online version of this article.

*Correspondence to: Kinji Ohno, Division of Neurogenetics, Center for Neurological Disease and Cancer, Nagoya University Graduate School of Medicine, 65 Tsurumai, Showa-ku, Nagoya 466-8550, Japan. E-mail: ohnok@med.nagoya-u.ac.jp

Contract grant sponsors: Ministry of Education, Culture, Sports, Science, and Technology of Japan, and the Ministry of Health, Labor, and Welfare of Japan.

AChE species. ColQ carries three domains: (1) an N-terminal proline-rich attachment domain that organizes the catalytic AChE subunits into a tetramer, (2) a collagen domain that forms a triple helix and contains heparin-binding domains, and (3) a C-terminal domain (CTD) enriched in charged residues and cysteines.

In previous studies, *COLQ* mutations were divided into four classes according to their positions in ColQ and their effects on the expression of AChE species in COS cells: (1) N-terminal mutations that prevent association of AChE_T with ColQ, (2) truncation mutations in the collagen domain that prevent the formation of ColQ-tailed AChE, (3) CTD missense mutations that prevent triple helical formation of ColQ, and (4) CTD mutations that do not abolish formation of ColQ-tailed AChE but affect anchoring of ColQ at the NMJ [Ohno et al., 2000]. We previously reported that p.Asp342Glu, p.Arg410Pro, and p.Arg410Glu, but not p.Cys444Tyr, at the CTD of ColQ compromise anchoring ColQ-tailed AChE to heterologous frog muscle sections [Kimbell et al., 2004]. We, however, did not show how the mutations affect anchoring of ColQ to the synaptic basal lamina. We also failed to prove pathogenicity of p.Cys444Tyr in the heterologous anchoring experiment. Two binding partners for anchoring ColQ-tailed AChE at the synaptic basal lamina have been reported to date: (1) the heparan sulfate proteoglycans such as perlecan, which bind to two heparan sulfate proteoglycan binding domains in the ColQ collagen domain [Arikawa-Hirasawa et al., 2002], and (2) the extracellular domain of MuSK, a muscle-specific receptor tyrosine kinase, on the postsynaptic membrane, which binds to the CTD of ColQ [Cartaud et al., 2004]. We recently demonstrated that anti-MuSK autoantibodies in patients with myasthenia gravis block binding of ColQ to MuSK [Kawakami et al., 2011]. We also reported that intravenous or intramuscular administration of adeno-associated virus serotype 8 (AAV8) carrying human *COLQ* efficiently anchors ColQ-tailed AChE at the NMJ [Ito et al., 2012]. We proved that ColQ-tailed AChE moves from one muscle to another and anchors to the synaptic basal lamina by exploiting the proprietary binding affinity for synaptic basal lamina, which we named the protein-anchoring therapy.

We here report three patients with AChE deficiency harboring *COLQ* mutations in the collagen domain and CTD. We examined the effects of the CTD mutations on interaction between ColQ and MuSK by in vitro and in vivo assays and found that the CTD mutations impair this interaction.

Materials and Methods

Patients

All human studies were performed under approvals of the institutional review boards of Nagoya University Graduate School of Medicine, National Center of Neurology and Psychiatry, Juntendo University Faculty of Medicine, and Utano National Hospital. Three patients participated in the study after appropriate informed consents were given. A mutation analysis had been done when they were 7, 12, and 19 years of age, respectively. All had respiratory distress or poor sucking at birth, slight delay in walking, fatigability since early childhood, normal intelligence, no anti-AChR and anti-MuSK antibodies, a decremental electromyographic response, repetitive CMAP to a single nerve stimulus, and no response to anticholinesterase medications (Table 1).

Mutation Analysis

Genomic DNA was isolated from blood with QIAamp Blood Mini Kit (Qiagen, Hilden, Germany). Poor response to anti-

cholinesterases suggested endplate AChE deficiency and slow channel syndrome. We thus directly sequenced 17 constitutive *COLQ* exons and their flanking regions with CEQ8000 sequencer (Beckman Coulter, Brea, CA). Names of all mutations were checked using Mutalyzer (<http://www.lovd.nl/mutalyzer/>). Identified mutations were submitted to an LSDB for the *COLQ* gene (<http://www.lovd.nl/COLQ>). As mutations were identified in *COLQ* in all the patients, we did not go into sequencing of *CHRNA1* (NM.00079.3; MIM #100690), *CHRN1* (NM.009601.4; MIM #100710), *CHRND* (NM.021600.2; MIM #100720), and *CHRNE* (NM.000080.3; MIM #100725) encoding the AChR α , β , δ , and ϵ subunits, respectively.

Construction of Expression Vectors

Human *ACHE_T*, *COLQ* cDNAs, and LacZ were cloned and introduced into a cytomegalovirus-based mammalian expression vector pTarget (Promega, Madison, WI) [Ohno et al., 1998]. Each mutation was introduced into *COLQ* cDNA using the QuikChange site-directed mutagenesis kit (Stratagene). The extracellular domain (aa 1–393) of human *MUSK* (NM.001166280.1; MIM #601296) cDNA (Open Biosystems/Thermo Scientific, Waltham, MA) was cloned into a mammalian expression vector pAptag-5 (GenHunter, Nashville, TN) at the *NbeI* and *XbaI* sites upstream of a myc epitope [Kawakami et al., 2011].

Transfection and AChE Extraction

Wild-type or mutant pTarget-*COLQ* was transfected into COS7 cells along with pTarget-*ACHE_T* in a 10-cm dish using XtremeGENE 9 DNA Transfection Reagent (Roche Diagnostics, Indianapolis, IN). Cells were incubated at 37°C for 48 hr and scraped from dish in Tris-HCl buffer (50 mM Tris-HCl [pH 7.0], 0.5% Triton X-100, 0.2 mM EDTA, 2 μ g/ml leupeptin, 1 μ g/ml pepstatin, and 0.1 μ mol/ml benzamide) containing 1 M NaCl. The extract was vortexed in a 1.5-ml tube and centrifuged at 14,000g for 5 min, and the supernatant was obtained.

Sedimentation Analysis

A sedimentation analysis was performed as previously described [Ohno et al., 1998]. The AChE-containing supernatant was applied on a 5%–20% sucrose density gradient, which was made in Tris-HCl buffer along with β -galactosidase (16.1 S) and alkaline phosphatase (6.1 S) as internal sedimentation standards. Centrifugation was performed in a Beckman SW41Ti rotor at 4°C for 21 hr at 178300g. The collected fractions were assayed for AChE activities using the Ellman method [Ellman et al., 1961] and determined the absorbance at 420 nm using a Sunrise Absorbance Reader (Tecan, Männedorf, Switzerland).

Isolation of ColQ-Tailed AChE on a Heparin-Agarose Column

For isolation of ColQ-tailed AChE, the extract was diluted in Tris-HCl buffer containing 0.2 M NaCl and loaded onto a HiTrap Heparin HP column (GE Healthcare, Buckinghamshire, UK). We washed the column with five volumes of Tris-HCl buffer containing 0.2 M NaCl, and eluted ColQ-tailed AChE with Tris-HCl buffer containing 1 M NaCl. We concentrated the eluate with an Amicon Ultra-4 Centrifugal Filter (50K) (Millipore, Billerica, MA) [Kawakami et al., 2011; Kimbell et al., 2004].

Table 1. Clinical Features and Mutations

Pt.	Sex	Age	Onset	Walking	Noc. NIV	Edrophonium i.v.	RNS	rCMAP	Exon	Nucleotide change	Amino-acid change
1	M	19 y	Birth	19 m	12 y	No change	-52%	+	11 14	c.679C>T c.965T>A	p.Arg227X p.Val322Asp
2	M	12 y	Birth	24 m	11 y	Respiratory distress	-32%	+	17	c.1339G>C ^a	p.Asp447His ^a
3	M	7 y	3 y	18 m	Not used	Improved	-79%	+	17 17	c.1331G>A c.1354C>T	p.Cys444Tyr p.Arg452Cys

^aHomozygous mutation.

Exon numbers are according to GenBank Accession NM_005677.3. Mutations are numbered according to NM_005677.3 (cDNA) and NP_005668.2 (protein). cDNA number +1 corresponds to the A of the ATG translation initiation codon.

Pt., patient; Noc. NIV, nocturnal noninvasive ventilation; RNS, repetitive nerve stimulation at 3 Hz of ulnar or accessory nerves; rCMAP, repetitive compound muscle action potential; m, months; y, years.

Transplantation of ColQ-tailed AChE to NMJs of *Colq*^{-/-} Mice

We obtained approvals of the *Colq*^{-/-} mice [Feng et al., 1999] studies by the Animal Care and Use Committee of the Nagoya University. We prepared 10- μ m-thick sections of quadriceps muscles of *Colq*^{-/-} mice with a Leica CW3050-4 cryostat at -20°C, and stored at -80°C until used. The muscle sections were fixed in acetone for 15 min. The stock solutions of ColQ-tailed AChE were diluted in Tris-HCl buffer containing 1 M NaCl and 5 mg/ml each of bovine serum albumin, chicken ovalbumin, and gelatin to give an Ellman unit equivalent to 1–2 ng of Torpedo AChE (Sigma, St. Louis, MO), and the NaCl concentration was adjusted to 0.5 M. To adjust the ionic strength of the solution, we added 50 mM Tris-HCl buffer stepwise over a period of 3 hr to 0.3 M NaCl. The slides were placed in a humidified chamber and incubated overnight at room temperature [Kimbell et al., 2004; Rotundo et al., 1997].

Immunofluorescence

For preparation of immunofluorescence, muscle sections were blocked with 5% horse serum in phosphate-buffered saline for 20 min. We detected ColQ-tailed AChE by anti-ColQ antibody [Ito et al., 2012] and anti rabbit-FITC secondary antibody at 1:100 (Vector Lab., Burlingame, CA), along with 2.5 μ g/ml Alexa-594-conjugated α -bungarotoxin (Sigma) for visualizing AChR. Signals of ColQ and AChR were examined with fluorescent microscope, BX60 (Olympus, Tokyo, Japan). We analyzed more than 10 muscle sections for each experiment and representative images are indicated in the figures.

Preparation of the Extracellular Domain of MuSK

pAptag-5 carrying hMuSKect-myc was transfected into HEK293 cells in a 10-cm dish using the calcium phosphate method. The hMuSKect-myc was purified with the c-myc-Tagged Protein Mild Purification Kit version 2 (MBL, Nagoya, Japan) [Kawakami et al., 2011].

In Vitro Plate-Binding assay for ColQ–MuSK Interaction

The Maxi-Sorp Immuno Plate (Nunc/Thermo Scientific) was coated with purified hMuSKect-myc at 4°C overnight and then blocked with phosphate-buffered saline containing 1% bovine serum albumin at room temperature for 1 hr. We incubated an equal Ellman unit of wild-type or mutant ColQ-tailed AChE at 4°C for 4 hr and then quantified the bound ColQ-tailed AChE by the Ellman method. Each time before we moved to the next step, we washed the plate three times with phosphate-buffered saline [Kawakami et al., 2011].

In Vivo Electroporation of pTarget-COLQ

The tibialis anterior muscles of *Colq*^{-/-} mice were injected with 50 μ g each of pTarget-COLQ and pTarget-LacZ plasmids. In vivo transfection was performed using an in vivo electroporator (CUY21EDIT; BEX Co., Ltd., Tokyo, Japan). A pair of electrode needles was inserted into the muscle in the longitudinal direction to a depth of 4 mm to encompass the plasmid-injected site. Pulses of 50 V and 25-msec were administered every 1 sec three times in forward polarity and three more times in the opposite polarity [Aihara and Miyazaki, 1998]. Seven days after the electroporation, mice were sacrificed and tibialis anterior muscles were analyzed.

AAV8-Mediated Expression of Mutant ColQ in *Colq*^{-/-} Mice

We prepared wild-type and mutant pAAV8-COLQ and intravenously administered them to *Colq*^{-/-} mice as described previously [Ito et al., 2012]. We inserted the wild-type human COLQ or mutant human COLQ harboring p.Asp447His into downstream of a CMV promoter in the pAAV-MCS vector using the AAV Helper-Free system (Stratagene). We employed AAV serotype 8 that can efficiently infect skeletal muscles. We injected 2 \times 10¹² vector genomes of wild-type or mutant pAAV-COLQ to the tail vein of 4-week-old male *Colq*^{-/-} mice. Similar copies of wild-type pAAV8-COLQ and mutant pAAV8-COLQ-p.Asp447His genomes were transduced into muscle cells with a mean ratio of 1.07 (mutant transgene/wild-type transgene, $n = 3$). We quantified motor functions up to 4 weeks after injection. Muscle weakness and fatigability were measured with a rotarod apparatus (Ugo Basile). Mice were allowed to take a rest for 1 hr between each rotarod task and an average of three measurements was taken. Spontaneous running-wheel activities were used to quantify voluntary exercises. Each mouse was placed in a standard cage equipped with a counter-equipped running wheel (diameter, 14.7 cm; width, 5.2 cm; Ohara Medical Corp., Tokyo, Japan). The running distances were recorded every 24 hr. At 6 weeks after injection, mice were sacrificed and sections of skeletal muscles were stained for AChR and ColQ to visualize the transduced ColQ-tailed AChE as described above.

Results

Mutation Analysis

On the basis of combined clinical and electrophysiological features such as early age of onset, negative response to cholinesterase inhibitors, respiratory insufficiency, and repetitive muscle response [Abicht et al., 2012; Engel, 2012], we first sequenced COLQ and identified that each patient carried two mutant COLQ alleles. Patient 1 had heterozygous [c.679C>T, p.Arg227X] +

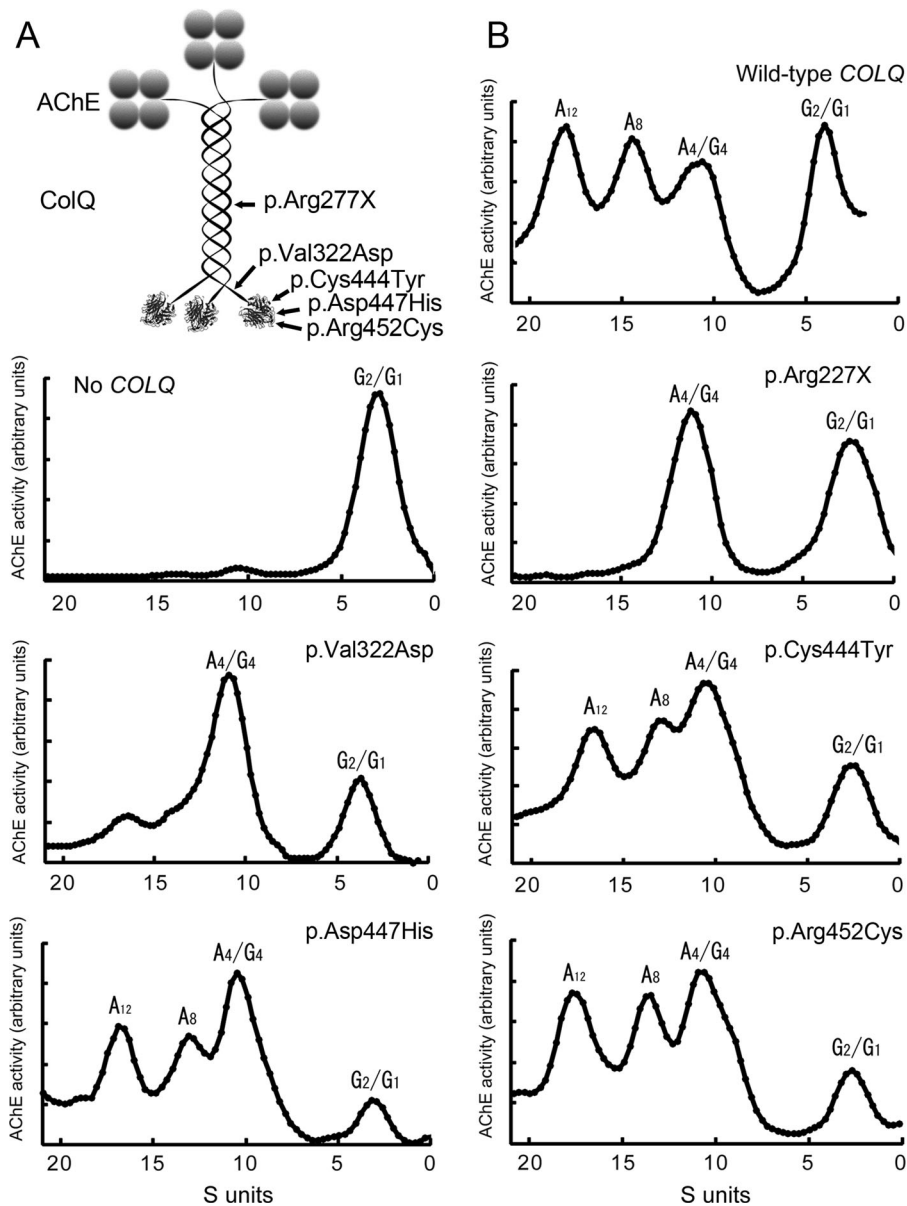


Figure 1. A: Schematic presentation of positions of the identified mutations in ColQ. **B:** Sedimentation profiles of AChE species extracted from COS cells transfected with wild-type *ACHE_T* cDNA and indicated *COLQ* cDNA. p.Arg227X is in the collagen domain, the other four missense mutations are in the C-terminal domain. p.Val322Asp has a small ~16-S peak (A₁₂ species), whereas the other missense mutations in the C-terminal region do not abolish formation of asymmetric AChE species. G₁, G₂, and G₄, globular forms; A₄, A₈, and A₁₂, asymmetric forms.

[c.965T>A, p.Val322Asp] mutations. Patient 2 was heterozygous for [c.1331G>A, p.Cys444Tyr] + [c.1354C>T, p.Arg452 Cys]. Patient 3 had a homozygous [c.1339G>C, p.Asp447His] mutation (Fig. 1A, Table 1, Supp. Fig. S1). We traced the mutations in the parents of patients 1 and 3, and found that the mutation on each allele was inherited from unaffected parents. In patient 2, we confirmed heterozygosity by cloning each allele of exon 17 and sequenced them. Among the five mutations, only c.1331G>A, p.Cys444Tyr was previously identified in another Japanese patient [Ohno et al., 2000], but its pathogenicity remained elusive [Kimbell et al., 2004]. The other four mutations were novel. All the amino acids at mutated codons were conserved across species [Ohno et al., 1998].

Sedimentation Profiles of Mutations

Four missense mutations were in CTD and the nonsense p.Arg227X was in the collagen domain. We first examined the effects of the mutations on formation of asymmetric ColQ-tailed AChE species in COS cells. The p.Arg227X mutation that truncates ColQ in its collagen domain did not produce normal A₁₂ species of ColQ-tailed AChE, as has been observed in other truncation mutations in the collagen domain [Ohno et al., 1998; 2000]. The p.Val322Asp mutation close to the N-terminal end of CTD similarly failed to produce A₁₂ species. By contrast, the other three CTD mutations (p.Cys444Tyr, p.Asp447His, and p.Arg452Cys) produced

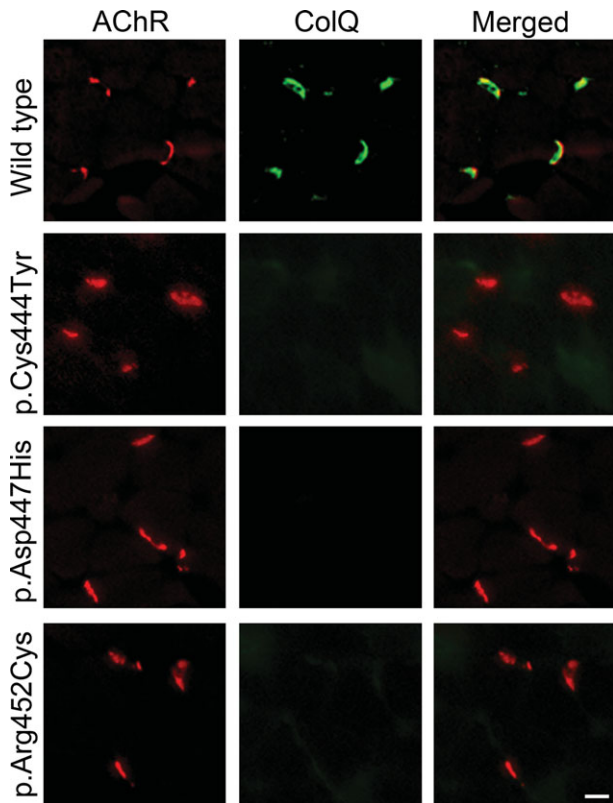


Figure 2. In vitro overlay assays. Plasmid encoding the indicated CTD mutations of human ColQ were cotransfected into COS cells together with a plasmid encoding the wild-type human AChE_T catalytic subunit. The A₁₂ AChE expressed in COS cells was isolated and overlaid on a 10- μ m quadriceps muscle section of *Colq*^{-/-} mice. ColQ-tailed AChE molecules harboring the indicated mutations do not colocalize with AChRs. ColQ is stained with anti-ColQ antibody and AChR with Alexa594-labeled α -bungarotoxin. Scale bar = 20 μ m.

normal or slightly reduced peaks of asymmetric A₄, A₈, and A₁₂ species compared to the wild-type (Fig. 1B).

Overlay of CTD Mutants to the NMJ of *Colq*^{-/-} Mice

We overlaid the purified recombinant human ColQ-tailed AChE protein complex on a section of skeletal muscle of *Colq*^{-/-} mice. Wild-type ColQ-tailed AChE colocalized with AChR at the NMJs, whereas ColQ-tailed AChE with p.Cys444Tyr, p.Asp447His, and p.Arg452Cys mutations failed to colocalize with AChR (Fig. 2). This assay showed that these CTD mutations impair anchoring of ColQ at the vertebrate NMJs.

In Vitro Plate-Binding Assay for ColQ–MuSK Interaction

As the synaptic anchorage of AChE by ColQ is partly dependent on the association of ColQ with MuSK [Cartaud et al., 2004], we next examined whether the CTD mutations had an effect on the interaction of human ColQ and human MuSK using an in vitro plate-binding assay. We coated the plate with purified hMuSKect-myc, and added a fixed amount of the purified recombinant human ColQ-tailed AChE protein complex. The bound AChE was quantified by the Ellman method. AChE activities of the CTD mutants carrying p.Cys444Tyr, p.Asp447His, and p.Arg452Cys were signif-

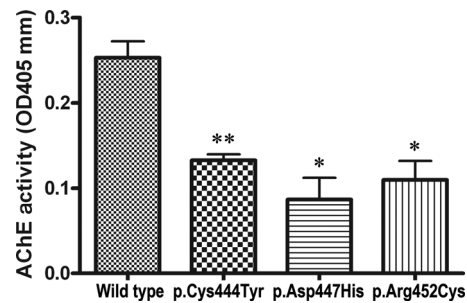


Figure 3. In vitro plate-binding assays. The extracellular domain of human MuSK (hMuSKect-myc) was coated on a 96-well plate. Purified recombinant ColQ-tailed AChE was overlaid on the plate. Bound ColQ-tailed AChE was quantified by AChE activity. **P* < 0.05, ***P* < 0.01 by Student's *t*-test.

icantly lower than that of wild-type CTD (Fig. 3). These results showed that impaired anchoring of the mutant ColQ-tailed AChE was due to the lack of interaction between ColQ and MuSK.

In Vivo Electroporation of *COLQ* with CTD Mutations into the Muscles of *Colq*^{-/-} Mice

To confirm whether the three CTD mutants indeed impair anchoring of ColQ-tailed AChE to the NMJ in vivo, we electroporated wild-type and mutant pTarget-*COLQ* constructs to tibialis anterior muscles of *Colq*^{-/-} mice. We first confirmed that the pTarget-LacZ plasmid is efficiently transduced into muscle fibers (Fig. 4A). ColQ-tailed AChE harboring p.Cys444Tyr, p.Asp447His, and p.Arg452Cys in CTD did not anchor to the NMJs of *Colq*^{-/-} mice (Fig. 4), although real-time RT-PCR revealed similar expression levels of the wild-type and mutant *COLQ* mRNAs (ranges of *COLQ/Gapdh* mRNAs = 0.03 to 0.11 for wild-type and three mutants). These studies revealed that the three mutant ColQ molecules were incompetent for anchoring to the NMJ in vivo.

AAV8-Mediated Expression of Mutant ColQ in *Colq*^{-/-} Mice

We previously reported the protein-anchoring therapy for *Colq*^{-/-} mice, in which ColQ-tailed AChE is moved to and anchored to remote NMJs using its proprietary binding affinities for perlecan and MuSK [Ito et al., 2012]. To directly prove that the CTD mutations compromise anchoring of ColQ to the NMJ in a model animal, we intravenously administered wild-type and p.Asp447His-mutant AAV8-*COLQ* to *Colq*^{-/-} mice, and analyzed motor functions and histological localization of ColQ. Motor functions evaluated by the dwell time on a rotarod (Fig. 5A) and by voluntary movements (Fig. 5B) were prominently improved in *Colq*^{-/-} mice treated with wild-type *COLQ* but not with p.Asp447His-*COLQ*. Histological studies similarly showed that ColQ was colocalized to AChR in *Colq*^{-/-} mice treated with AAV-wild-type *COLQ* but not with AAV-p.Asp447His-*COLQ* (Fig. 5C).

Discussion

CMSs have a variety of causes that lead to defects in the NMJ signal transmission. Elucidation of the molecular pathomechanisms is essential to develop and provide a specific treatment for CMS patients. Ephedrine and albuterol are effective for patients with

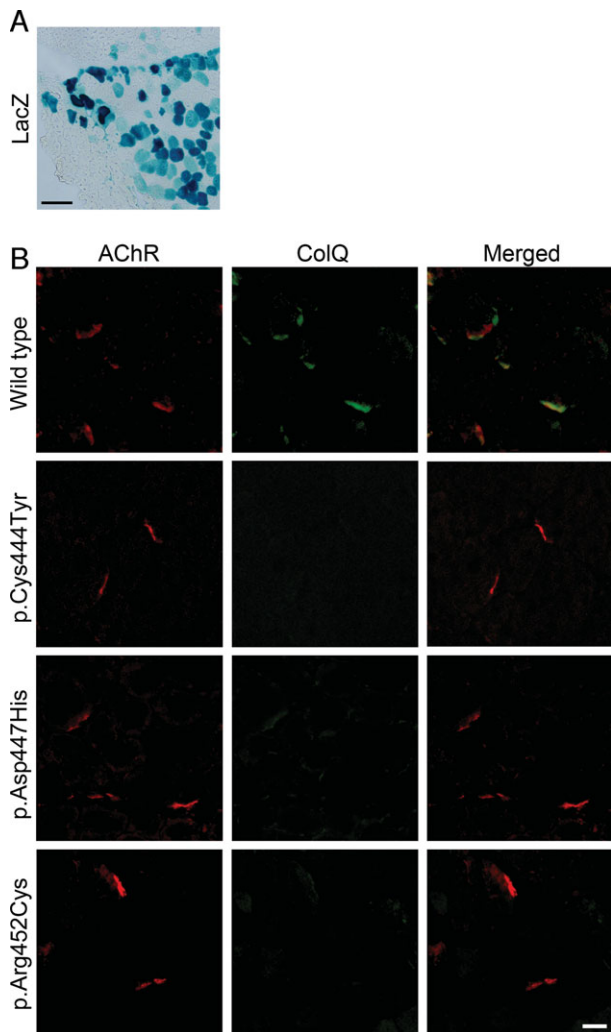


Figure 4. In vivo electroporation. **A:** Histochemical staining for β -galactosidase activity in the muscle after gene transfer of pTarget-lacZ with electroporation. The transverse section of the muscle was stained with X-gal. **B:** Immunocytochemistry using serial muscle sections showed that ColQ-tailed AChE molecules harboring p.Val322Asp, p.Asp447His, p.Cys444Tyr, and p.Arg452Cys in ColQ, do not colocalize with AChRs in tibialis anterior muscles of *Colq*^{-/-} mice. ColQ is stained with anti-ColQ antibody and AChR with Alexa594-labeled α -bungarotoxin. Scale bar = 100 μ m (**A**) and 20 μ m (**B**).

endplate AChE deficiency harboring *COLQ* mutations [Chan et al., 2012; Engel et al., 2010]. Cholinesterase inhibitors cannot improve neuromuscular transmission and often worsen myasthenic symptoms and respiratory conditions. Therefore, an early genetic diagnosis is important for the patients. Clinical features of the three patients prompted us to search for mutations in *COLQ*, and indeed we detected five *COLQ* mutations. Four of them are novel and p.Cys444Tyr has been previously reported in another Japanese patient [Ohno et al., 2000]. It is interesting to note that the five mutations are unique to Japanese patients, which suggests that all the mutations have recently arisen in the patients' families and are unlikely to be founder mutations.

In 1998, we cloned human *COLQ* cDNA, identified its genomic structure, and detected *COLQ* mutations in patients with endplate AChE deficiency [Ohno et al., 1998]. We also proved that mutations in the collagen domain impair formation of ColQ-tailed

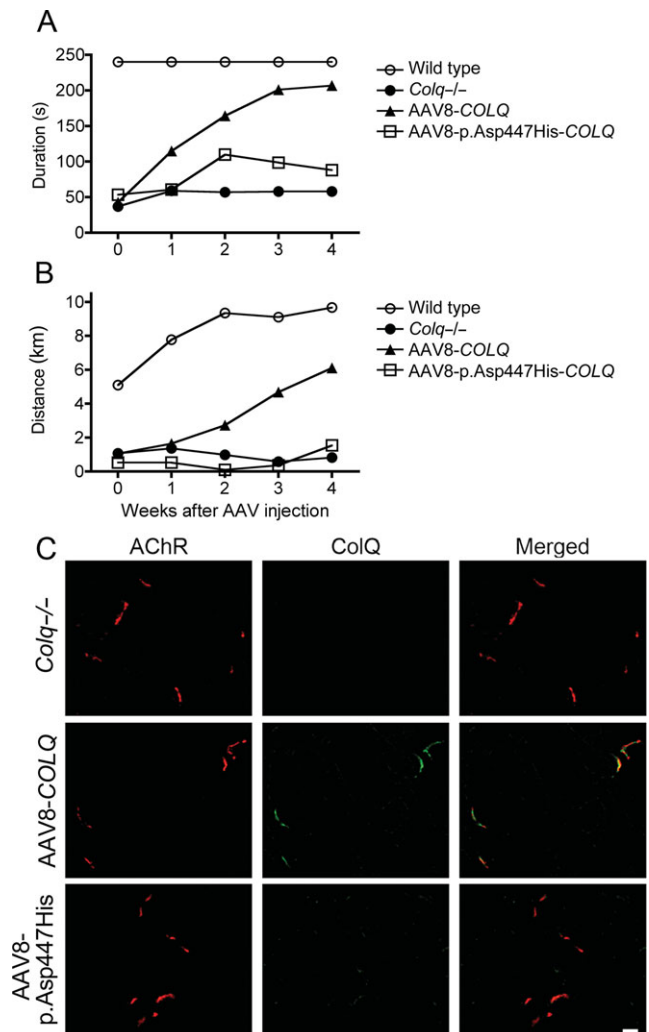


Figure 5. AAV8-mediated expression of mutant ColQ in *Colq*^{-/-} mice. **A:** Temporal profiles of dwell times on a rotarod that linearly accelerated from 0 to 40 rpm in 240 sec. **B:** Voluntary movements per day were quantified with a counter-equipped running wheel. **C:** Visualization of ColQ-AChE and AChR on the section of skeletal muscle using anti-ColQ antibody and α -bungarotoxin, respectively. AAV8-*COLQ*-p.Asp447His failed to anchor ColQ-tailed AChE to the NMJ. Scale bar = 20 μ m.

AChE [Ohno et al., 1998]. We later reported four classes of *COLQ* mutations as stated in the introduction, and proved pathogenicity in three classes but not in a class comprising CTD mutations [Ohno et al., 1999; 2000]. We next proved pathogenicity of five mutations (p.Arg315X, p.Asp342Glu, p.Gln371X, p.Arg410Gln, and p.Arg410Pro) in CTD using the heterologous overlay of human ColQ-tailed AChE to the frog muscles, but another mutation, p.Cys444Tyr, had no effect on anchoring of ColQ to the frog NMJ [Kimbell et al., 2004]. To summarize, we have reported 23 *COLQ* mutations and have succeeded in proving the pathogenicity in 22 mutations [Kimbell et al., 2004; Ohno et al., 1998; 1999; 2000; Shapira et al., 2002]. p.Cys444Tyr in CTD has thus been the only mutation that we failed to prove why the patient was deficient for AChE. Donger et al. (1998) reported p.Tyr430Ser in CTD in a patient with endplate AChE deficiency, but the sedimentation analysis yielded normal asymmetric species of AChE. The p.Tyr430Ser mutation was later employed to prove that CTD binds to MuSK by immunoprecipitation experiments [Cartaud et al., 2004]. Four

additional mutations (p.Arg341Gly, p.Cys386Ser, p.Cys417Tyr, and p.Thr441Ala) in CTD have been reported by others but none have been functionally analyzed [Mihaylova et al., 2008; Muller et al., 2004].

In the present study, we found four missense mutations (p.Val322Asp, p.Asp447His, p.Cys444Tyr, and p.Arg452Cys) in CTD and one truncation mutation (p.Arg227X) in the collagen domain in three patients with endplate AChE deficiency. Three mutations (p.Val322Asp, p.Asp447His, and p.Arg452Cys) in CTD have not been functionally characterized and one was p.Cys444Tyr, for which the pathogenicity remained elusive. We characterized the functional consequences of these mutations.

The analysis of sedimentation profiles revealed that p.Arg227X and p.Val322Asp abolish formation of normal asymmetric A₁₂ species of AChE. p.Val322Asp is the only mutation that affects formation of A₁₂ and is the only mutation that introduces a negatively charged residue in CTD. We previously reported that 1082delC in CTD introduces 64 hydrophobic missense residues after the frameshift, which prevents triple helix formation [Ohno et al., 2000]. CTD is enriched with prolines, cysteines, and charged residues. The hydrophobicity profile is likely to be essential in CTD. p.Val322Asp introduces a hydrophilic aspartate residue, and disrupts a hydrophobic cluster close to the N-terminal end of CTD (Supp. Fig. S2A). Prediction of a secondary structure similarly demonstrates shortening of a β -sheet and de novo insertion of a turn before an α -helix (Supp. Fig. S2B). We do not observe these gross alterations in predicted structures with p.Cys444Tyr, p.Asp447His, and p.Arg452Cys (Supp. Fig. S2). p.Val322Asp is thus likely to compromise the tertiary structure of CTD and leads to defective triple helix formation.

The analysis of sedimentation profiles showed that the other CTD mutations, p.Cys444Tyr, p.Asp447His, and p.Arg452Cys, generated normal asymmetric A₁₂ species of AChE. We next examined the anchoring competence of these mutations. We had previously employed frog muscles to analyze anchoring incompetence of CTD mutations, but failed to prove it for p.Cys444Tyr [Kimbell et al., 2004]. We thus used the vertebrate NMJs of *Colq*^{-/-} mice, and proved that all three mutations are not able to anchor to the mouse NMJ. Anchoring competence of p.Cys444Tyr to frog NMJs but not to mouse NMJs suggests that p.Cys444Tyr does not grossly change the conformation of CTD and is likely to be a mild mutation. Indeed, the onset of patient 3 carrying p.Cys444Tyr was at the age of 3 years, and the patient started walking at 18 months, which are the mildest among the three currently analyzed patients.

To further dissect the underlying molecular bases of anchoring incompetence of p.Cys444Tyr, p.Asp447His, and p.Arg452Cys, we quantified the ColQ–MuSK interaction by the in vitro plate-binding assay, which enabled us to estimate the binding affinities of these two molecules. The three missense mutations decreased the activities of ColQ-tailed AChE bound to MuSK to ~50% or less, which suggests that ~50% reduction of the binding affinity is likely to be required to compromise anchoring of ColQ to the NMJ.

Moreover, we demonstrated the pathogenicity of the mutations in a model animal for the first time. We electroporated the three CTD mutations into tibialis anterior muscles of *Colq*^{-/-} mice, and found that each mutation was indeed anchoring-incompetent. To further prove the pathogenicity of one of the mutations in *Colq*^{-/-} mice, we intravenously injected AAV8-COLQ-p.Asp447His to *Colq*^{-/-} mice and found that motor deficits remained essentially the same and anchoring of ColQ was not observed at the NMJs.

In vitro plate-binding assays revealed ~50% reduction of binding affinity of ColQ for MuSK for p.Cys444Tyr, p.Asp447His, and p.Arg452Cys (Fig. 3), but these mutants were not at all anchored to the NMJ by in vitro overlay assay (Fig. 2), in vivo electroporation

(Fig. 4), and AAV8 treatment (Fig. 5). Among the three mutants, p.Cys444Tyr showed the most preserved binding affinity for MuSK, which, however, was not sufficient to anchor the mutant ColQ to the NMJ in in vitro overlay assay (Fig. 2) and in vivo electroporation (Fig. 4). The presence of heparan sulfate proteoglycans like perlecan at the NMJ in these assays was unlikely to sufficiently compensate for the defective CTD–MuSK interaction, which also underscores a pivotal role of CTD–MuSK interaction on binding of ColQ to the NMJ. Although the same amount of ColQ-tailed AChE was used for in vitro plate-binding and in vitro overlay assays, the amount of MuSK (>150 ng/well) used in in vitro plate-binding assay was likely to be much more than that at the NMJ in in vitro overlay assay, which may account for the difference in up to 50% preservation of ColQ binding in in vitro plate-binding assay and complete lack of ColQ binding in in vitro overlay assay.

Acknowledgments

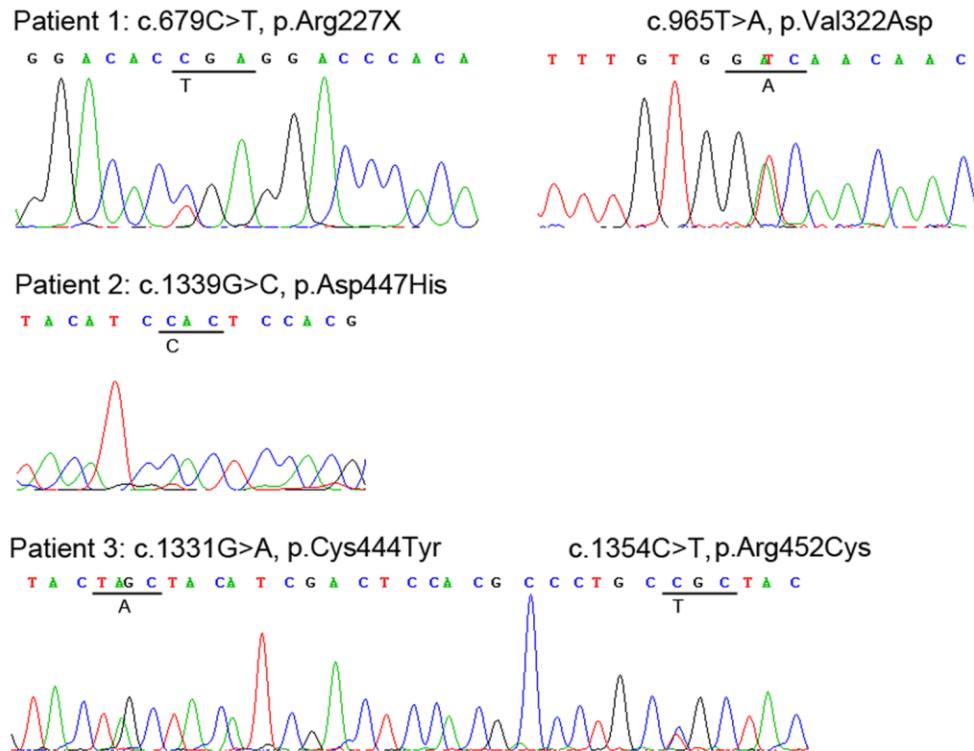
We thank Yasutaka Ohya, Kumiko Yano, and Koji Nomaru at Division for Research of Laboratory Animals of Nagoya University for technical assistance.

Disclosure statement: The authors declare no conflict of interest.

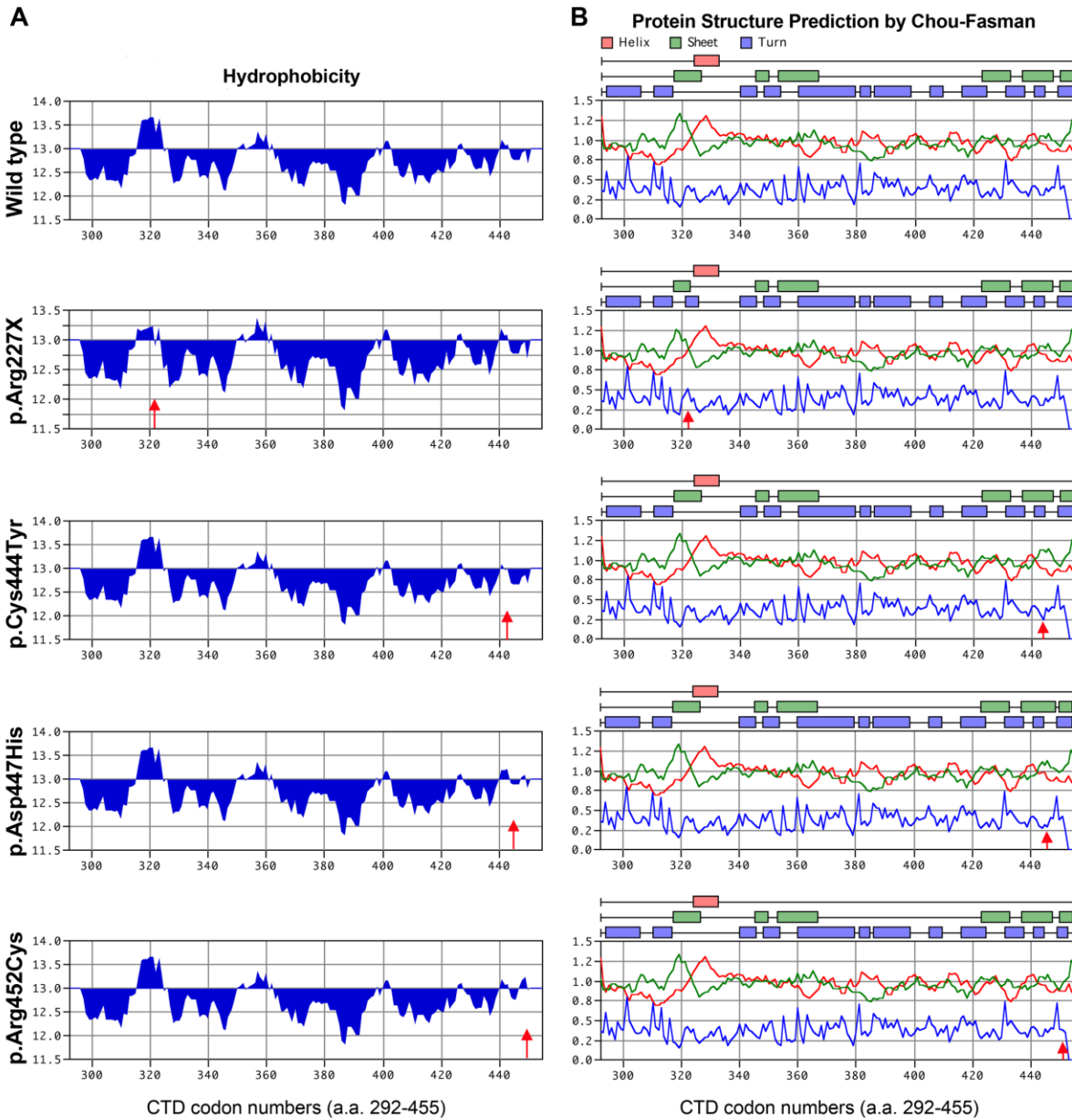
References

- Abicht A, Dusl M, Gallenmuller C, Guerguelcheva V, Schara U, Della Marina A, Wibbeler E, Almaras S, Mihaylova V, von der Hagen M, Huebner A, Chaouch A, et al. 2012. Congenital myasthenic syndromes: achievements and limitations of phenotype-guided gene-after-gene sequencing in diagnostic practice: a study of 680 patients. *Hum Mutat* 33:1474–1484.
- Aihara H, Miyazaki J. 1998. Gene transfer into muscle by electroporation in vivo. *Nat Biotechnol* 16:867–870.
- Arikawa-Hirasawa E, Rossi SG, Rotundo RL, Yamada Y. 2002. Absence of acetylcholinesterase at the neuromuscular junctions of perlecan-null mice. *Nat Neurosci* 5:119–123.
- Cartaud A, Strohlich L, Guerra M, Blanchard B, Lambergeon M, Krejci E, Cartaud J, Legay C. 2004. MuSK is required for anchoring acetylcholinesterase at the neuromuscular junction. *J Cell Biol* 165:505–515.
- Chan SH, Wong VC, Engel AG. 2012. Neuromuscular junction acetylcholinesterase deficiency responsive to albuterol. *Pediatr Neurol* 47:137–140.
- Donger C, Krejci E, Pou Serradell A, Eymard B, Bon S, Nicole S, Chateau D, Gary F, Fardeau M, J, M, Guicheney P. 1998. Mutation in the human acetylcholinesterase-associated collagen gene, *COLQ*, is responsible for congenital myasthenic syndrome with end-plate acetylcholinesterase deficiency (Type Ic). *Am J Hum Genet* 63:967–975.
- Ellman GL, Courtney KD, Andres V, Jr, Feather-Stone RM. 1961. A new and rapid colorimetric determination of acetylcholinesterase activity. *Biochem Pharmacol* 7:88–95.
- Engel AG. 2012. Congenital myasthenic syndromes in 2012. *Curr Neurol Neurosci Rep* 12:92–101.
- Engel AG, Lambert EH, Gomez MR. 1977. A new myasthenic syndrome with end-plate acetylcholinesterase deficiency, small nerve terminals, and reduced acetylcholine release. *Ann Neurol* 1:315–330.
- Engel AG, Ohno K, Sine SM. 2003. Sleuthing molecular targets for neurological diseases at the neuromuscular junction. *Nat Rev Neurosci* 4:339–352.
- Engel AG, Shen XM, Selcen D, Sine SM. 2010. What have we learned from the congenital myasthenic syndromes. *J Mol Neurosci* 40:143–153.
- Feng G, Krejci E, Molgo J, Cunningham JM, Massoulié J, Sanes JR. 1999. Genetic analysis of collagen Q: roles in acetylcholinesterase and butyrylcholinesterase assembly and in synaptic structure and function. *J Cell Biol* 144:1349–1360.
- Ito M, Suzuki Y, Okada T, Fukudome T, Yoshimura T, Masuda A, Takeda S, Krejci E, Ohno K. 2012. Protein-anchoring strategy for delivering acetylcholinesterase to the neuromuscular junction. *Mol Ther* 20:1384–1392.
- Kawakami Y, Ito M, Hirayama M, Sahashi K, Ohkawara B, Masuda A, Nishida H, Mabuchi N, Engel AG, Ohno K. 2011. Anti-MuSK autoantibodies block binding of collagen Q to MuSK. *Neurology* 77:1819–1826.
- Kimbell LM, Ohno K, Engel AG, Rotundo RL. 2004. C-terminal and heparin-binding domains of collagen tail subunit are both essential for anchoring acetylcholinesterase at the synapse. *J Biol Chem* 279:10997–11005.

- Massoulié J. 2002. The origin of the molecular diversity and functional anchoring of cholinesterases. *Neurosignals* 11:130–143.
- Mihaylova V, Muller JS, Vilchez JJ, Salih MA, Kabiraj MM, D'Amico A, Bertini E, Wolffe J, Schreiner F, Kurlmann G, Rasic VM, Siskova D, et al. 2008. Clinical and molecular genetic findings in COLQ-mutant congenital myasthenic syndromes. *Brain* 131:747–759.
- Muller JS, Petrova S, Kiefer R, Stucka R, Konig C, Baumeister SK, Huebner A, Lochmuller H, Abicht A. 2004. Synaptic congenital myasthenic syndrome in three patients due to a novel missense mutation (T441A) of the COLQ gene. *Neuropediatrics* 35:183–189.
- Ohno K, Brengman J, Tsujino A, Engel AG. 1998. Human endplate acetylcholinesterase deficiency caused by mutations in the collagen-like tail subunit (ColQ) of the asymmetric enzyme. *Proc Natl Acad Sci USA* 95:9654–9659.
- Ohno K, Brengman JM, Felice KJ, Cornblath DR, Engel AG. 1999. Congenital endplate acetylcholinesterase deficiency caused by a nonsense mutation and an A→G splice-donor-site mutation at position +3 of the collagenlike-tail-subunit gene (COLQ): how does G at position +3 result in aberrant splicing? *Am J Hum Genet* 65:635–644.
- Ohno K, Engel AG, Brengman JM, Shen X-M, Heidenrich FR, Vincent A, Milone M, Tan E, Demirci M, Walsh P, Nakano S, Akiguchi I. 2000. The spectrum of mutations causing endplate acetylcholinesterase deficiency. *Ann Neurol* 47:162–170.
- Rotundo RL, Rossi SG, Anglister L. 1997. Transplantation of quail collagen-tailed acetylcholinesterase molecules onto the frog neuromuscular synapse. *J Cell Biol* 136:367–374.
- Shapira YA, Sadeh ME, Bergtraum MP, Tsujino A, Ohno K, Shen XM, Brengman J, Edwardson S, Matoth I, Engel AG. 2002. Three novel COLQ mutations and variation of phenotypic expressivity due to G240X. *Neurology* 58:603–609.
- Sigoillot SM, Bourgeois F, Lambergeon M, Strohlic L, Legay C. 2010. ColQ controls postsynaptic differentiation at the neuromuscular junction. *J Neurosci* 30:13–23.



Supp. Figure S1. Sequence chromatograms showing *COLQ* mutations. Codon units are underlined. Mutant nucleotides are shown below each nucleotide.



Supp. Figure S2. Hydrophobicity profiles of wild-type and mutant CTDs. Positions of mutations are indicated by red arrows. **A:** p.Val322Asp introduces a hydrophilic aspartate residue and attenuates a hydrophobic cluster close to the N-terminal end of CTD, while the other mutations minimally change the hydropathy profiles. **B:** Chou-Fasman prediction of CTD secondary structures. p.Val322Asp causes shortening of a β -sheet and *de novo* insertion of a turn before an α -helix, whereas the other mutations do not grossly change the predicted structures.